



Development of an electrochemical sensor for environmental pollutant detection based on cobalt sulfide and graphene nanocomposite

Neda Babaee Dezfouli ^a, Zhila Safari ^{*a}, Halimeh Rajabzadeh ^a

^a Department of Chemistry, Dez.C., Islamic Azad University, Dezfoul, Iran

ARTICLE INFO

Article history:

Received: 30 April 2025

Accepted: 20 June 2025

Available online: 25 June 2025

Keywords:

Cobalt Sulfide

Cobalt Sulfide-Graphene
Nanocomposite

Electrocatalytic Oxidation

Hydrazine



(CC BY 4.0)

Copyright © 2025 by the author(s)

ABSTRACT

Hydrazine is a toxic and carcinogenic substance that can enter the human body through multiple pathways, leading to poisoning and other adverse health effects. Given its ecological significance in various aqueous environments and its widespread industrial applications, accurate quantification and monitoring of hydrazine in environmental systems are crucial. Electroanalytical techniques for hydrazine assessment demonstrate considerable promise owing to their cost-effectiveness, exceptional detection limits, and rapid analytical response. In this study, a new, simple, and cost-effective electrode is proposed and presented for the measurement of hydrazine. This electrode is a modified electrode based on a nanocomposite composed of cobalt sulfide and graphene nanoparticles. The modified cobalt sulfide-graphene electrode, after preparation, was used as a nanocomposite sensor for the electrocatalytic measurement of hydrazine through cyclic voltammetry. Due to the presence of nanoparticles in its structure, this electrode exhibits sensitivity and selectivity in the electroanalysis of hydrazine. The effects of various parameters, such as scan rate (from 10 to 300 mV/s), pH (from 3 to 10), and different concentrations of hydrazine (from 0.2 to 2 mM), were investigated. The nanocomposite was characterized using field emission scanning electron microscopy (FESEM). To determine the diffusion coefficient of hydrazine, chronoamperometry techniques were used, and the diffusion coefficient of hydrazine in this study was calculated to be 8.48×10^{-9} cm²/s. The detection limit was determined using differential pulse voltammetry, calculated to be 0.081 mM.

Highlights

- A novel cobalt sulfide-graphene nanocomposite electrode was proposed for electrocatalytic hydrazine sensing.
- The presence of nanoparticles ensured high sensitivity and selectivity in hydrazine electroanalysis.
- The proposed sensor achieved a low limit of detection (0.081 mM) via Differential Pulse Voltammetry (DPV).
- The diffusion coefficient of hydrazine was determined as 8.48×10^{-9} cm²/s using chronoamperometry.

1. Introduction

Electrochemical sensing platforms are highly regarded for their numerous advantages, including ease of use, cost-effectiveness, high specificity, and improved detection capabilities. As a result, these devices have become essential analytical tools in various fields, such as food quality control, environmental monitoring, clinical diagnostics, biomedical evaluation, and counterterrorism security. Electrochemical sensors are mainly categorized into three types: amperometric, potentiometric, and impedimetric. The development of new electrode substrates with enhanced charge transport properties,

structural durability, and larger active surface areas is crucial for maximizing the effectiveness of electrochemical sensing systems (Fazeli-Nasab et al., 2022; Meng et al., 2024).

In contemporary scientific research, ultrathin planar nanomaterials particularly graphene-based architectures have garnered considerable attention owing to their exceptional physicochemical characteristics and versatile utility in electronic components, photonic devices, catalytic systems, and electrochemical energy storage solutions. These atomically layered materials have become pivotal in the evolution of next-generation electrochemical sensing

* Corresponding author.

E-mail address: Zhilasafari@yahoo.com

<https://doi.org/10.22034/aes.2025.532560.1107>

platforms. The expansive interfacial domain of graphene nanostructures enables exceptional analyte adsorption capacity, facilitating ultra-sensitive detection. Furthermore, the abundant surface functionalities on modified graphene variants permit diverse strategies for immobilizing biorecognition elements, enabling precise electrochemical interrogation of biomacromolecules such as proteins and oligonucleotides. Significant research efforts have been devoted to developing advanced hybrid nanocomposites through strategic material integration for enhanced sensor applications (Iqbal et al., 2024; Traipop et al., 2024).

A recent study utilized electropolymerization through repetitive potential cycling to immobilize a synthetic recognition layer onto an unmodified graphite substrate. This functionalized transducer was then used for trace-level quantification of lead. The fabrication process took place under ambient conditions, with optimal analytical performance observed at pH 8.0 using Britton-Robinson buffer as the supporting electrolyte. Comprehensive electrochemical characterization was conducted using cyclic voltammetry and differential pulse voltammetry, while high-resolution electron microscopy was employed to assess the topological features (Wang et al., 2022).

In a study (Motaharian and Milani, 2015), A novel voltammetric detection platform was engineered utilizing a molecularly imprinted polymer (MIP)-functionalized carbon composite electrode for selective quantification of the benzodiazepine compound diazepam. The synthetic recognition elements were fabricated through precipitation-induced polymerization protocol and subsequently integrated as the bioactive interface in the electrochemical transducer assembly. Comparative analytical evaluation revealed the MIP-modified carbon composite electrode exhibited significantly enhanced molecular recognition capability for diazepam compared to its non-imprinted polymer (NIP) counterpart. The developed biosensing platform demonstrated successful application in detecting therapeutic concentrations of diazepam in complex biological matrices, specifically human blood serum specimens.

It has been conducted (Najafi and Sohuli, 2018) research on the development of a sensor for fentanyl determination. This investigation developed a novel electroanalytical platform through functionalization of a glassy carbon substrate with multi-walled carbon nanostructures and ferric oxide nanoparticles for ultrasensitive fentanyl detection in aqueous media. The engineered transducer's surface architecture was characterized using high-resolution field emission scanning electron microscopy. Electrochemical characterization was conducted through cyclic potential sweeps, while quantitative analysis employed pulsed potential techniques. The optimized sensor demonstrated dual linear response ranges (80 nM - 1 μ M and 1 - 100 μ M) for fentanyl quantification, achieving a remarkably low detection threshold of 45 nM. The anodic oxidation current showed excellent correlation with analyte concentration across both dynamic ranges, confirming the platform's robust performance for opioid monitoring.

It has been developed (Wang et al., 2007) it has been developed an innovative voltammetric biosensing platform utilizing polypeptide-graphenic nanodot heterostructures as dual signal-enhancing components for precise quantification of hydrosoluble micronutrients in commercial dietary supplements. The study pioneered the electrochemical polymerization of biocompatible polystyrene-graphenic nanodot hybrids as an advanced interfacial engineering approach for glassy carbon electrode functionalization, creating a novel electroanalytical interface. Through potential-controlled synthesis employing cyclic voltammetric deposition (1.5-2.0 V potential window), quantum-confined carbon nanostructures were successfully immobilized on polycarboxylate matrices, as confirmed by high-resolution field emission microscopy demonstrating stable nanodot dispersion within the polymeric network. The engineered transducer exhibited exceptional electrocatalytic activity, enabling sensitive detection of target micronutrients via both cyclic and differential pulse voltammetric techniques, with the nanocomposite architecture significantly enhancing analytical performance through synergistic signal amplification mechanisms.

It has been conducted a novel multiplexed electrochemical detection platform through electrosynthetic polymerization of conductive β -cyclodextrin-based macromolecular networks onto reduced graphene-functionalized screen-printed transducers. The engineered biosensing interface exhibited outstanding analytical performance for the simultaneous quantification of ascorbate, dopamine, and urate biomarkers. The supramolecular polymeric film showed excellent signal reproducibility and long-term operational stability. The crosslinked β -cyclodextrin architecture's host-guest recognition capabilities, paired with the enhanced electron transfer properties of the reduced graphene substrate, facilitated the selective and simultaneous detection of all three electroactive analytes in complex matrices (Ping et al., 2012). It has been employed (Golabi et al., 2001) a vitreous carbon electrode functionalized with pyrocatechol violet (PCV) for the electrochemical catalysis of hydrazine oxidation. The investigation utilized cyclic voltammetric analysis to derive kinetic parameters, achieving a quantification threshold of 4.2 micromolar for hydrazine detection.

2. Materials and methods

The experimental electrochemical analysis was conducted utilizing an Autolab PGSTAT028N potentiostat-galvanostat system integrated with a conventional three-electrode electrochemical cell interfaced with computational data acquisition software. The electrochemical cell configuration comprised: (i) a Metrohm-sourced saturated silver/silver chloride (Ag/AgCl/KCl) reference electrode, (ii) a high-purity graphite rod serving as the counter electrode, and (iii) a platinum substrate functioning as the modified working electrode, with the latter being fabricated in-house. All electrode potentials were standardized against the Ag/AgCl reference electrode. The raw voltammetric data acquired by

the potentiostat were subsequently exported to spreadsheet software for quantitative analysis and graphical representation (Nigde et al., 2022).

2.1. Preparation of cobalt sulfide-graphene (CoS₂-GR) nanocomposite

Graphene oxide (GO) is a single-layer structure derived from graphite oxide, which is essentially a graphite base sheet interspersed with epoxy and hydroxyl functional groups, along with carbonyl and carboxyl groups at the edges. Graphite oxide does not occur naturally and is synthetically produced. Since producing pure graphene is relatively difficult and expensive, graphene derivatives, such as graphene oxide, are used for its production. The fundamental distinction between graphitic oxide and graphenic oxide resides in their lamellar architecture—graphitic oxide exists as a multilamellar stacked system, while graphenic oxide comprises isolated or oligolamellar sheets. This structural divergence gives graphenic oxide unique advantages, especially as a transitional precursor for synthesizing monoatomic or few-atomic-layer graphene matrices. The material has garnered significant scientific interest due to its exceptional physicochemical properties, such as enhanced surface reactivity and tunable electronic characteristics, which result from its reduced dimensionality compared to multilayered graphene. Additionally, graphene oxide functions as an electrical insulator and enhances the tensile strength of composite materials by disrupting the connections within the graphene network (Uzdrowska et al., 2025).

The fabrication of CoS₂-graphene hybrid nanostructures began with the preparation of graphene oxide (GO) nanosheets through a modified Hummers oxidation process. The resulting GO powder was then subjected to ultrasonic exfoliation in 80 mL of ultrapure

water (18.2 M Ω -cm resistivity) to create a homogeneous colloidal dispersion. Stoichiometric amounts of cobalt(II) chloride hexahydrate (2 mmol) and thiourea (4 mmol) were added to this aqueous suspension as metal and sulfur precursors, respectively. The reaction mixture was then sonicated for 60 minutes to ensure thorough homogenization. Following this, the precursor solution was transferred to a PTFE-lined stainless steel hydrothermal reactor for solvothermal treatment at 453 K (180°C) for 24 hours under autogenous pressure. After cooling to ambient temperature (298 K), the reaction products were isolated by centrifugation at 10,000 rpm. The resulting black nanocomposite sediment was purified through multiple washing cycles with deionized water and absolute ethanol to remove any residual reactants. Finally, the product was dried under reduced pressure (10⁻² Torr) at 333 K (60°C) for 24 hours to yield the desired CoS₂-GR nanocomposite (Huo et al., 2024).

2.2. Characterization of cobalt sulfide-graphene nanoparticles

Field emission scanning electron microscopy (FESEM) images and energy-dispersive X-ray spectroscopy (EDX) results from the SEM analysis of cobalt sulfide-graphene nanoparticles are shown in Figure 1 and 2. The FESEM images reveal a uniform dispersion of interconnected nanoparticles on the graphene surface, which is attributed to the electrostatic attraction between the cobalt sulfide nanoparticles and the graphene surface. This electrostatic attraction leads to a uniform distribution on the final surface (Choi et al., 2024). The FESEM images indicate that the sheets have an average diameter of 30 nanometers. EDX analysis confirms the presence of sulfur, cobalt, and carbon atoms in the sample.

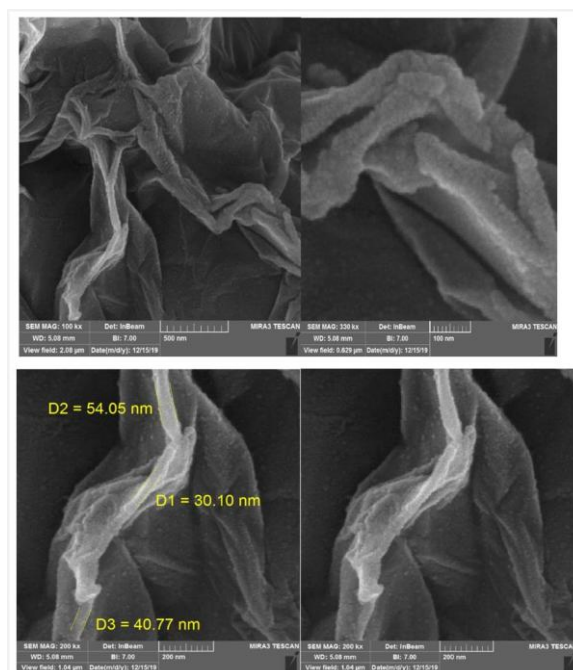


Figure 1. High-resolution FESEM micrograph depicting the surface topography of cobalt sulfide-decorated graphene hybrid nanostructures.

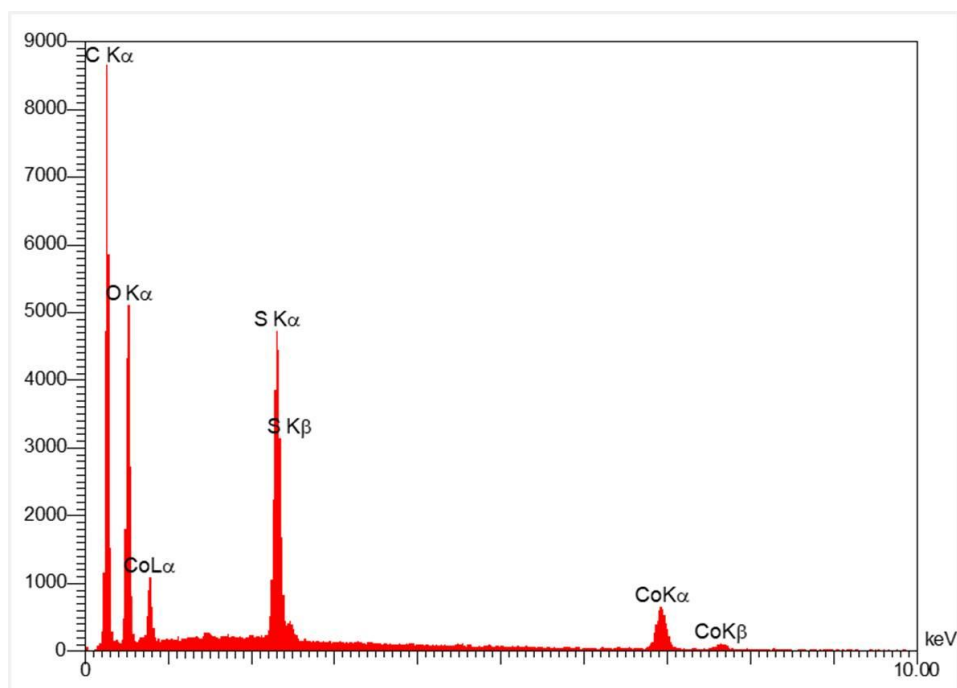


Figure 2. EDX elemental analysis spectra confirming the composition of cobalt sulfide-graphene nanocomposites.

2.3. Immobilization of the nanocomposite material on the working electrode

To prepare the suspension for electrode modification, 10.0 mg of the dry CoS_2 -GR nanocomposite powder was dispersed in 1.0 mL of deionized water via 30 minutes of ultrasonication to form a homogeneous 10 mg mL^{-1} suspension. For electrode modification, a $5 \mu\text{L}$ aliquot of the well-dispersed CoS_2 -GR suspension (10 mg mL^{-1}) was precisely pipetted and deposited at the center of the pristine platinum working electrode surface, resulting in a total nanocomposite loading of $50 \mu\text{g}$. The solvent was allowed to evaporate under ambient conditions for 20 to 25 minutes, forming a uniform thin-film coating of the nanocomposite on the electrode surface. Following complete solvent evaporation, the modified electrode was rinsed gently with deionized water to remove any loosely adsorbed material and was subsequently used for electrochemical characterization.

2.4. Hydrazine measurement method using cyclic voltammetry

Cyclic voltammetry is an advanced potentiostatic technique derived from linear potential sweep methodology. It involves applying a time-dependent triangular waveform potential to the working electrode, alternating between oxidative and reductive polarization. This widely used electroanalytical method is essential for gaining mechanistic insights into charge transfer processes, particularly during the initial characterization of novel electrochemical systems. Its significance stems from the direct quantitative relationship between faradaic peak current density and the concentration of electroactive analytes, making it the most versatile and comprehensive method for investigating redox-active species. Its operational flexibility and straightforward experimental setup have led to its widespread adoption in various

electrochemical research fields, including inorganic coordination complexes, organic redox systems, and biomolecular electron transfer processes. In the voltammetry method, three electrodes are used: the working electrode, the reference electrode, and the auxiliary electrode. The potential is applied between the working and reference electrodes, while the current is measured between the working and auxiliary electrodes (Bourgeois, 2001). In this system, the three electrodes are connected to a galvanostat. The working electrode, along with the other two electrodes, is placed in different solutions, and an appropriate potential and sweep rate depending on the type of experiment are applied. In this way, it was used for all experiments, including determining the optimal pH, examining the effect of sweep rate on electrochemical behavior, concentration effect, and determining hydrazine in various samples.

3. Results

This investigation aims to engineer an advanced electrochemical transducer through surface functionalization, establishing a robust analytical protocol for hydrazine quantification with enhanced sensitivity, precision, rapid response, operational simplicity, and economic viability. To elucidate the electrochemical behavior and quantify the active surface area of both pristine and functionalized electrodes, cyclic voltammetric analysis was conducted in a reversible redox probe system utilizing potassium ferrocyanide ($\text{K}_4[\text{Fe}(\text{CN})_6]$). The experimental protocol involved immersing both electrode variants in 10 mM ferrocyanide electrolyte and executing potential sweeps across a scan rate spectrum of $10\text{-}300 \text{ mV s}^{-1}$ (refer to Figures 3-4). Distinct oxidation and reduction peaks corresponding to the $[\text{Fe}(\text{CN})_6]^{3-/4-}$ redox couple were evident for both electrodes, with notably augmented current densities observed on the cobalt sulfide-graphene

nanocomposite modified surface. These observations align with the Randles-Ševčík theoretical framework, which predicts linear dependence of peak current on the square root of scan rate for diffusion-controlled reversible systems (Herbei et al., 2023; Mirceski et al., 2024). The linearity of this graph confirms that the electron transfer process on the surface of the modified electrode is diffusion-controlled and that the active surface area of the modified electrode has increased (Figures 5 and 6).

The voltammetric profiles shown in Figures 5 and 6 illustrate a notable reduction in peak potential separation

(ΔE_p) for the functionalized electrode compared to its unmodified version. This decrease in polarization potential is directly linked to improved charge transfer kinetics at the nanostructured interface, indicating enhanced electrochemical reversibility due to the modified surface architecture. The lower ΔE_p value quantitatively confirms the increased electron transfer efficiency achieved through electrode functionalization, as the catalytic nanocomposite layer effectively lowers activation barriers for the redox process.

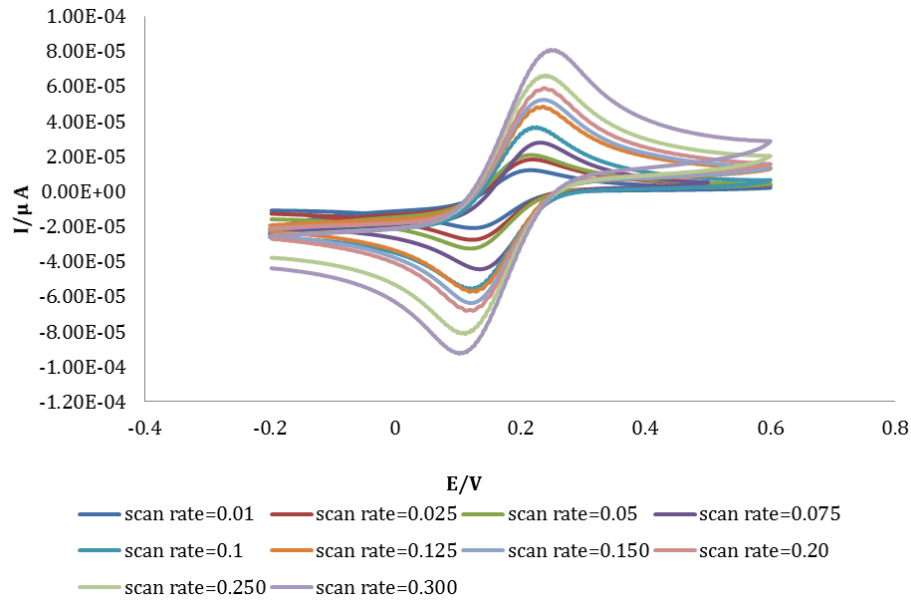


Figure 3. Cyclic voltammetry profiles of $K_4[Fe(CN)_6]$ at varying potential sweep rates using a bare (unmodified) electrode.

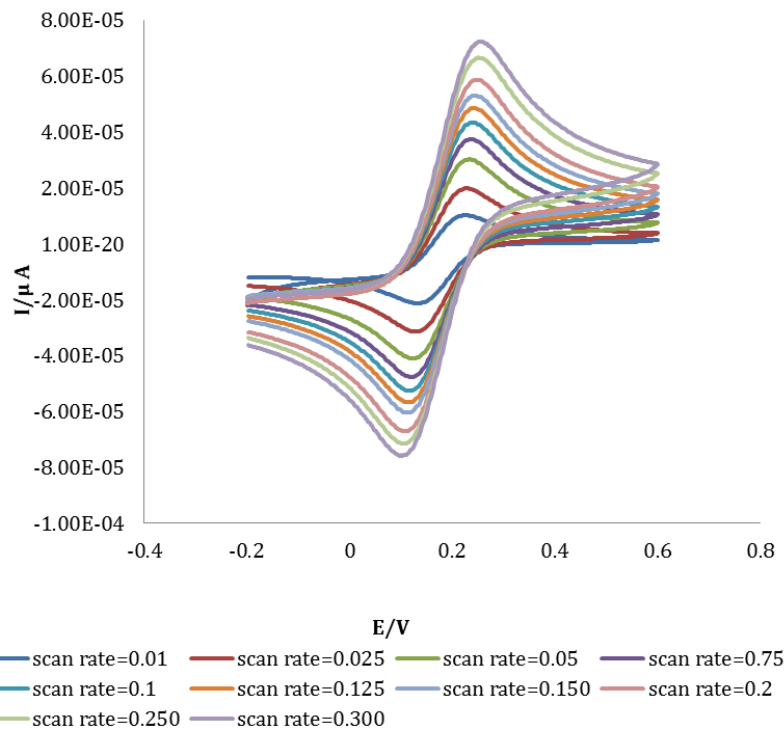


Figure 4. Cyclic voltammetric response of $K_4[Fe(CN)_6]$ at multiple scan rates on a cobalt sulfide-graphene modified electrode.

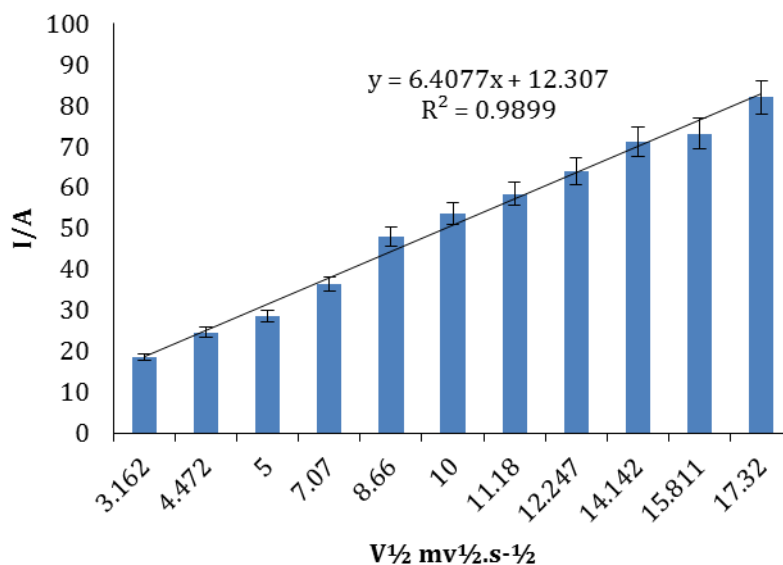


Figure 5. Linear correlation between anodic peak current and the square root of scan rate for the unmodified electrode.

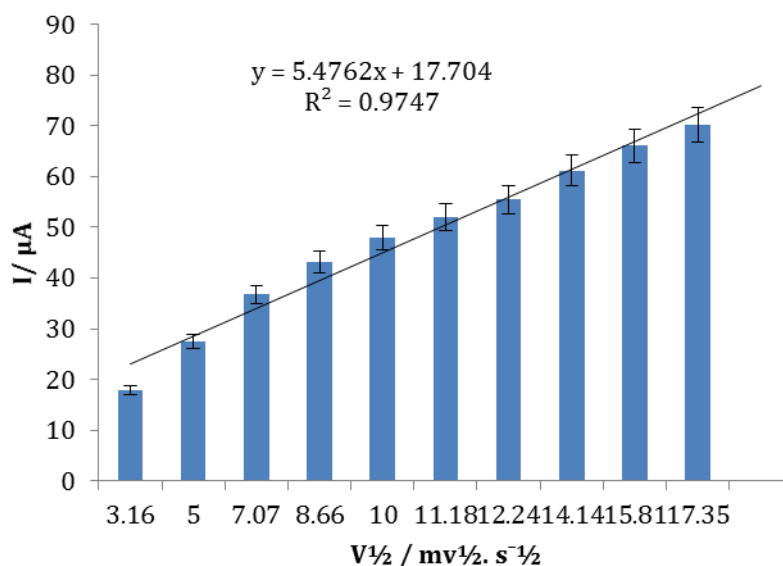


Figure 6. Dependence of anodic peak current on the square root of scan rate for the cobalt sulfide-graphene functionalized electrode.

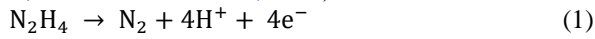
The operational durability of the cobalt disulfide-graphene hybrid material was assessed through continuous cyclic voltammetric scanning over 50 cycles in a potassium ferrocyanide electrolyte (Figure 7). The electrochemical analysis revealed remarkable stability, with both oxidation and reduction potentials showing negligible shifts ($\Delta E < 5$ mV) throughout the testing period. Quantitative evaluation indicated only a minimal current decrease of $3.8 \pm 0.2\%$ in peak current density, confirming the excellent structural integrity and interfacial adhesion of the nanocomposite coating. These results highlight the exceptional electrochemical robustness of the surface-bound cobalt sulfide-graphene nanostructure under repeated redox cycling conditions.

The electrochemical behavior of the modified electrode was systematically investigated as a function of nanocomposite loading concentration, given the critical

influence of material composition on charge transfer kinetics. Voltammetric characterization was performed using electrodes functionalized with 5 μL and 10 μL aliquots of cobalt disulfide-graphene nanohybrid suspension in potassium ferrocyanide electrolyte. Comparative analysis of oxidative peak currents revealed superior electrocatalytic activity for the 5 μL modified electrode, which was consequently selected as the optimal configuration for subsequent experiments.

A systematic evaluation of hydrazine electrooxidation pathways was conducted through cyclic voltammetric analysis of 2 mM hydrazine solutions across varying pH conditions (Figure 9). The voltammetric profiles revealed a cathodic shift in oxidation potential concomitant with increasing alkalinity, accompanied by moderate current enhancement at pH 9. Optimal electrocatalytic performance was observed at pH 9, demonstrating

maximum faradaic current density. The oxidation potential exhibited a non-monotonic dependence on pH, increasing progressively from pH 6 to 9 before decreasing at more alkaline conditions. This characteristic potential-pH relationship suggests a proton-coupled electron transfer mechanism governed by the following redox process: The observed electrochemical behavior confirms that hydrazine oxidation within the pH 6-9 window proceeds through a concerted proton-electron transfer process involving stoichiometric equivalence of both species. (Golabi et al., 2001; Michalkiewicz et al., 2024):



Cyclic voltammetric analysis was employed to investigate the electrocatalytic oxidation kinetics of hydrazine (2 mM) at a cobalt disulfide-graphene

nanocomposite-modified electrode (Profile α), with comparative studies performed on an unfunctionalized electrode (Profile β) and a background control in hydrazine-free phosphate buffer (Profile γ), all measurements conducted under standardized conditions (pH 9, 50 mV/s scan rate) as depicted in Figure 10. The nano-hybrid-modified surface demonstrated significantly enhanced electrochemical activity, evidenced by pronounced current amplification and favorable potential shifts relative to the unmodified substrate, while the control measurement established the baseline electrochemical signature of the supporting electrolyte system (Karami-Kolmoti and Zaimbashi, 2023).

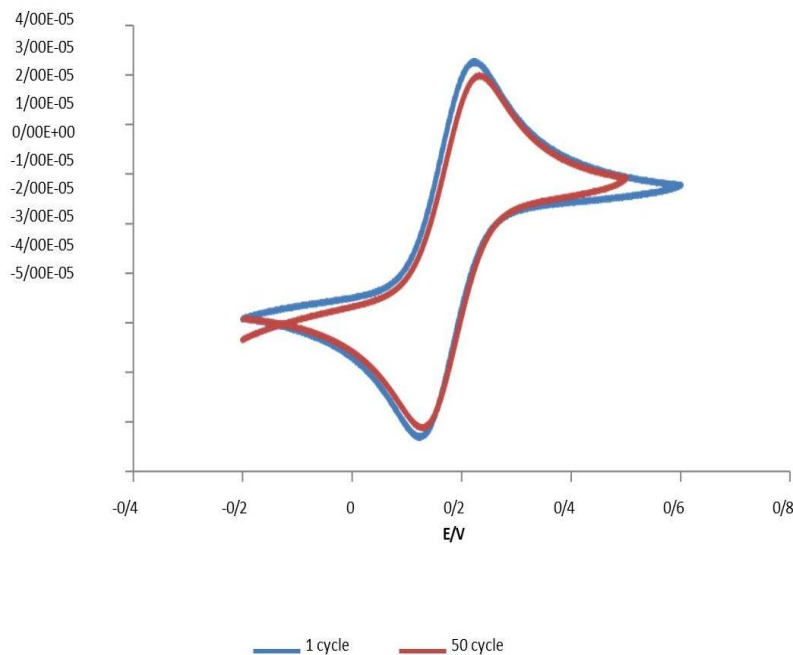


Figure 7. Successive cyclic voltammetry scans of $\text{K}_4[\text{Fe}(\text{CN})_6]$ at 50 mV/s using the cobalt sulfide-graphene nanocomposite-modified electrode.

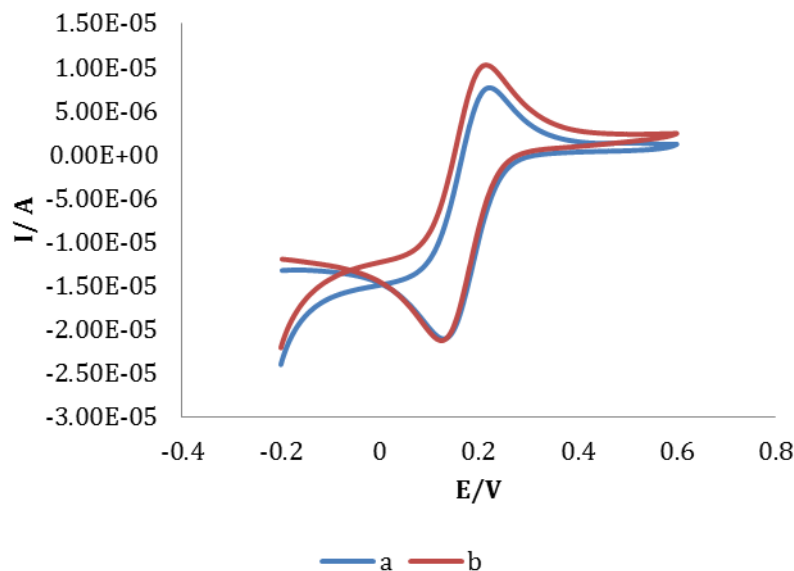


Figure 8. Comparative electrode modifications: (a) 10 μL deposition, (b) 5 μL deposition.

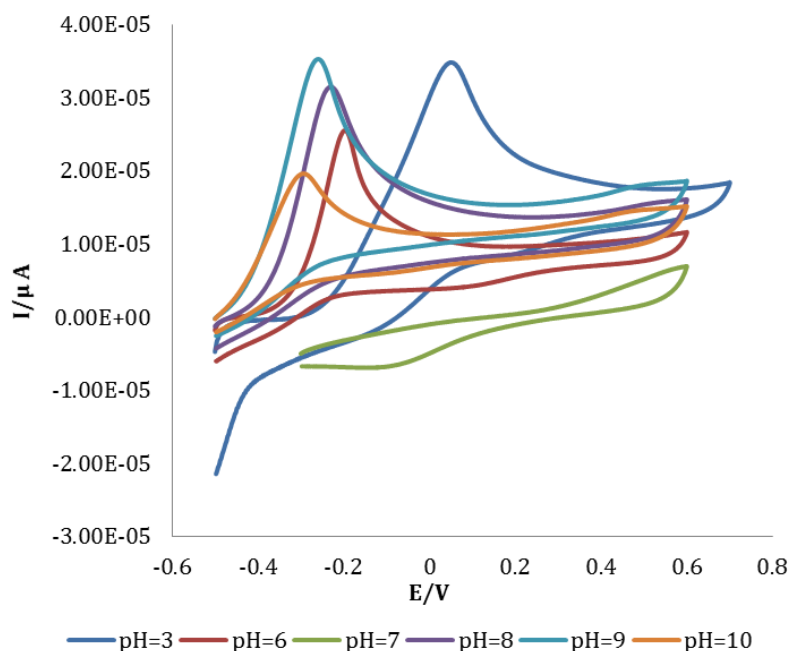


Figure 9. pH-dependent cyclic voltammetric behavior of hydrazine solutions.

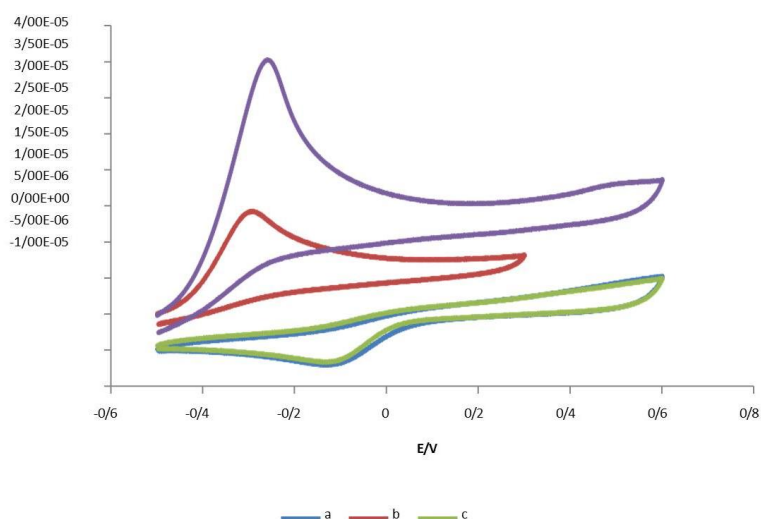


Figure 10. Comparative CV responses in pH 9 phosphate buffer: (a) Modified electrode with 2 mM hydrazine, (b) Unmodified electrode with 2 mM hydrazine, (c) Unmodified electrode (blank).

The voltammetric response of the functionalized electrode was characterized across multiple scan rates in pH 9 phosphate buffer electrolyte containing 2 mM hydrazine. Subsequent quantitative analysis revealed a linear correlation ($R^2 > 0.99$) between oxidative peak current density and the square root of scan rate (Figure 11), demonstrating diffusion-controlled charge transfer kinetics at the nanostructured interface. This relationship confirms the electrochemical reaction follows the Randles-Ševčík behavior, where mass transport limitations dominate the redox process at the modified electrode surface.

To determine the diffusion coefficient of hydrazine (D) on the nanoparticle-modified electrode, we employed chronoamperometry. A potential of 300 mV relative to the reference electrode was applied, and chronoamperograms

were recorded under optimal conditions for various concentrations of hydrazine. Based on the Cottrell equation, the variation of current as a function of the inverse square root of time was plotted for different concentrations of hydrazine over a specific time range (Figure 12). The slope value for each concentration was obtained, and according to the Cottrell relationship, it was observed that the variation of current with the inverse square root of time is linearly diffusion-controlled (Figure 13) (Sheikh-Mohseni and Pirsā, 2016).

Next, the graph of the variation in the slopes of the $I - t^{-\frac{1}{2}}$ lines in Figure 13 and 14 were plotted against the concentration of hydrazine. From the slope of this graph, the diffusion coefficient of hydrazine was found to be $8.48 \times 10^{-9} \text{ cm}^2 \text{ s}^{-1}$.

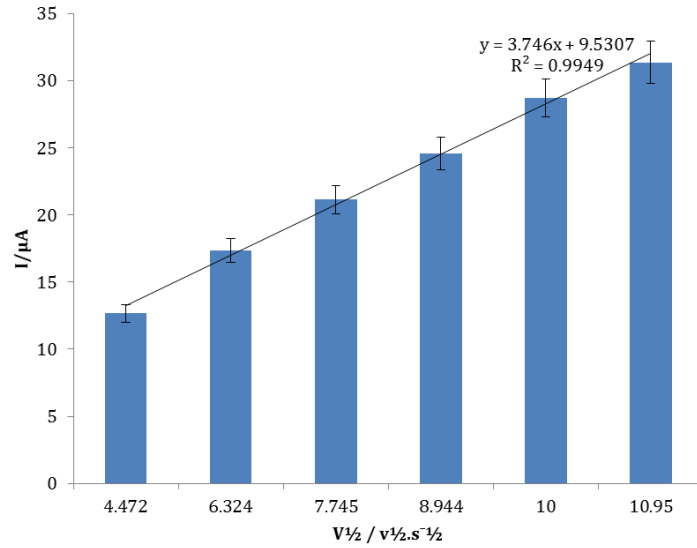


Figure 11. Chronoamperometric recordings of the modified electrode in pH 9 buffer with incremental hydrazine concentrations

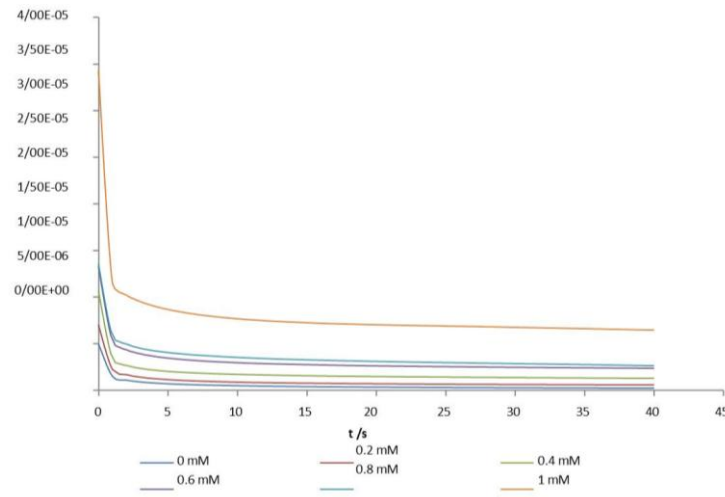


Figure 12. Chronoamperograms of the modified electrode in a buffer solution with pH = 9 in the presence of different concentrations of hydrazine.

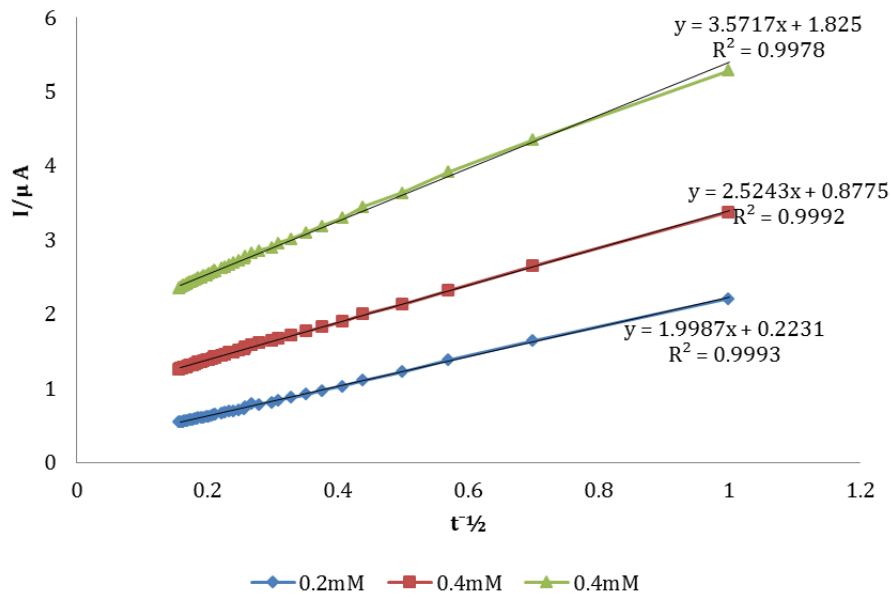


Figure 13. Cottrell plot (current vs. $t^{-1/2}$) for varying hydrazine concentrations in pH 9 buffer.

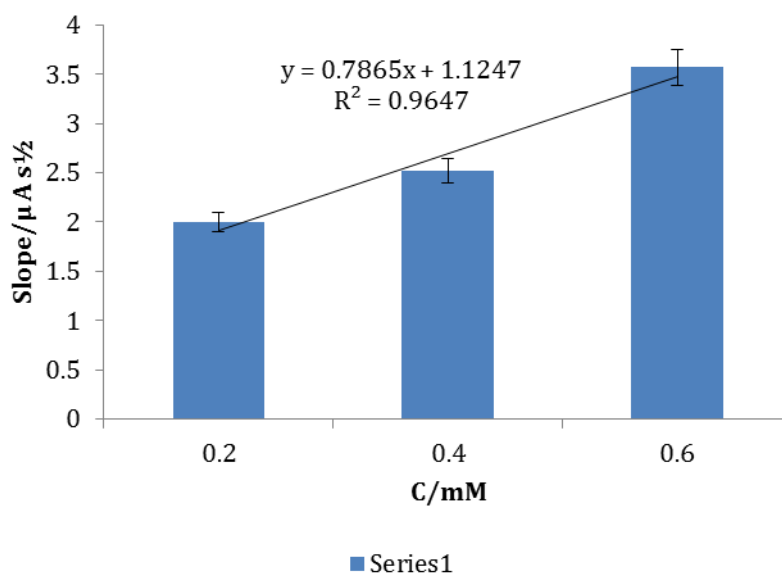


Figure 14. Slope analysis of $I-t^{-1/2}$ linear regressions as a function of hydrazine concentration.

Differential pulse voltammetry (DPV) was chosen as the primary analytical method because it offers superior resolution and increased sensitivity compared to traditional voltammetric techniques. This method allowed for the accurate development of a calibration profile and the determination of the hydrazine detection threshold. Quantitative analysis was performed under optimized conditions (applied potential: -0.6 to -0.1 V vs. reference, pH 9 phosphate buffer electrolyte) using a nanostructured electrode. The voltammetric response showed a linear relationship between oxidative current amplitude and

hydrazine concentration within the 0.1-2 mM range. The progressive augmentation of anodic peak intensity with increasing analyte concentration ($\Delta I/\Delta C = 12.3 \mu\text{A}/\text{mM}$, $R^2 = 0.998$) confirms both the electrochemical stability of the cobalt disulfide-graphene nanocomposite and its sustained catalytic activity during successive analyte introduction. This behavior substantiates the material's potential for continuous monitoring applications requiring stable electrocatalytic performance (Figure 15) (Karami-Kolmoti and Zaimbashi, 2023).

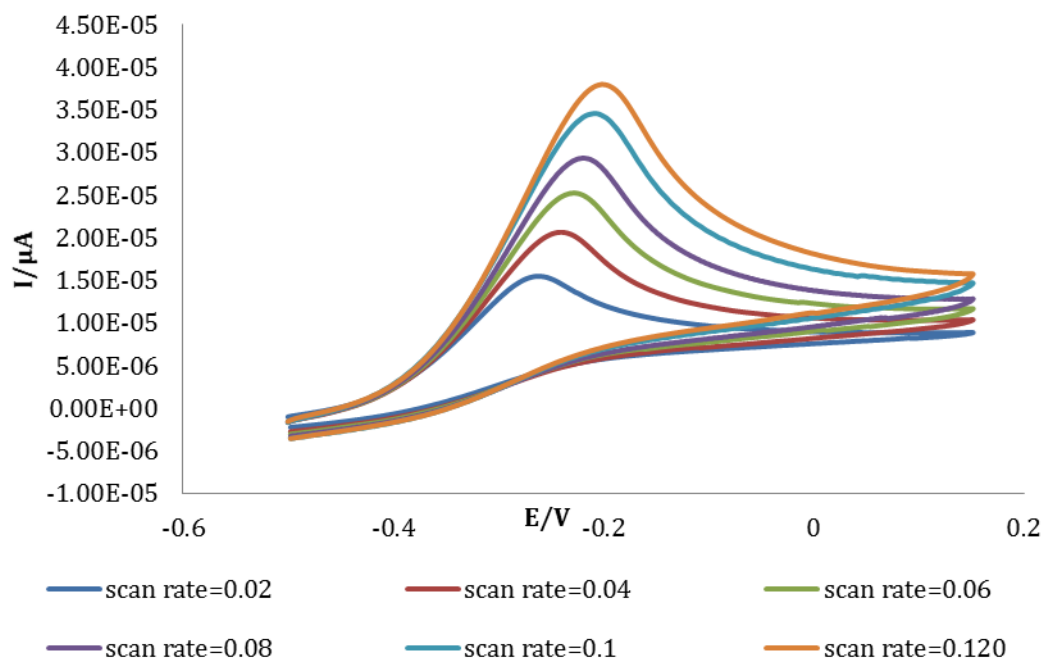


Figure 15. Anodic peak current vs. square root of scan rate for the nanocomposite-modified electrode.

In Figures 16 and 17, the peak current of the differential pulse voltammogram is shown as a function of hydrazine concentration. The calibration curve for hydrazine is linear in the concentration range of 0.2 to 2 mM. In this concentration range, the sensitivity is $0.0051 \mu\text{A}/\mu\text{M}$. At higher concentrations of hydrazine, the generation of nitrogen gas at the electrode surface increases and affects

the diffusion of hydrazine. Therefore, the slope of the calibration curve decreases at higher concentrations. The gas production at lower concentrations is not sufficient to hinder the diffusion of hydrazine toward the electrode. From the slope of the calibration curve, the detection limit of the sensor for hydrazine was calculated to be 0.081 mM.

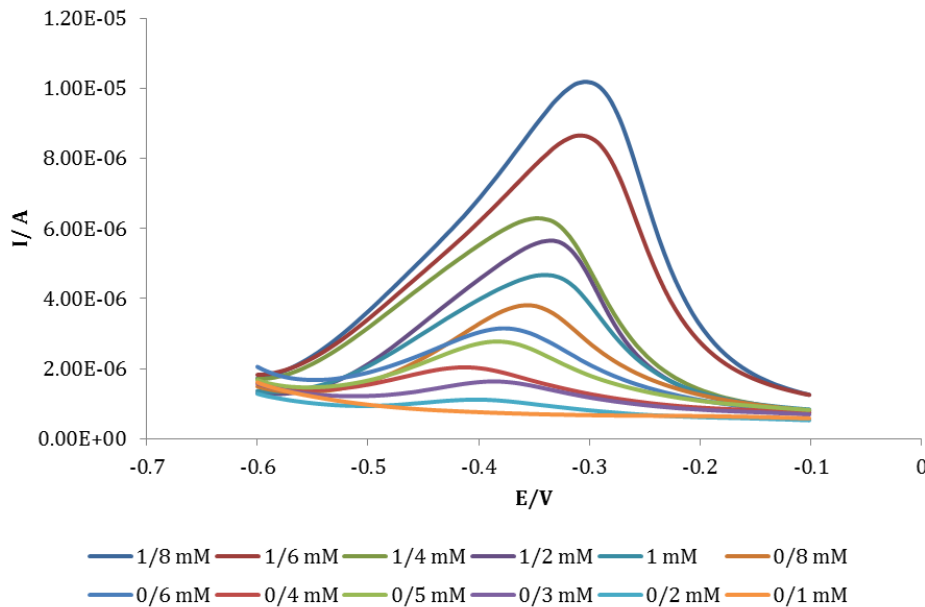


Figure 16. Differential pulse voltammetry responses for hydrazine detection at different concentrations (pH 9 buffer).

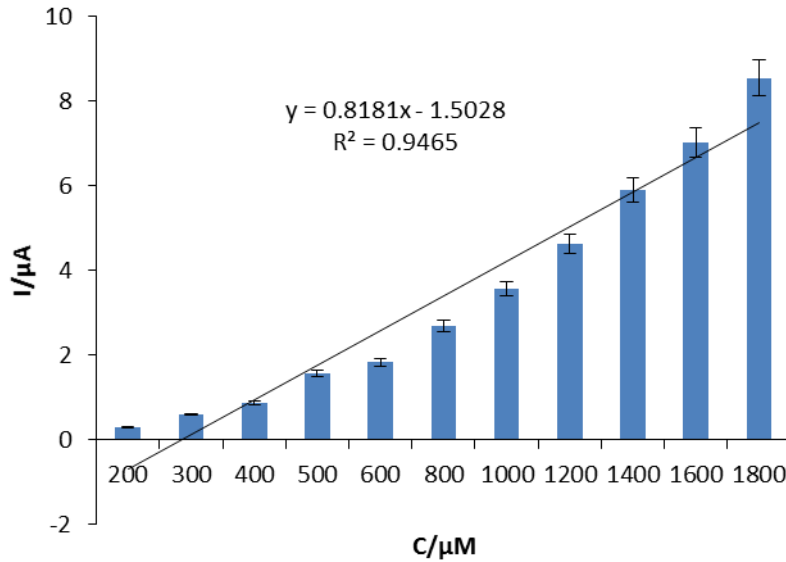


Figure 17. Standard calibration curve for hydrazine quantification (0.2–2 mM range)

4. Discussion

According to Nicholson's theory, the peak potential separation (ΔE_p) of a reversible redox couple serves as an important indicator of electron transfer kinetics at the electrode surface. The relationship demonstrates an inverse correlation between ΔE_p and the electron transfer rate constant (k^0) - as k^0 increases, the ΔE_p value decreases correspondingly. This fundamental principle arises because faster electron transfer kinetics allow the redox system to

maintain equilibrium more effectively during potential scanning, resulting in narrower peak separation. The theoretical foundation for this relationship is based on the Butler-Volmer formalism of electrode kinetics. In this framework, rapid electron transfer enables efficient charge propagation across the electrode-electrolyte interface. When the standard rate constant (k^0) is sufficiently high—typically greater than 0.1 cm/s for a one-electron process—the system exhibits nearly reversible behavior,

characterized by minimal peak separation (ΔE_p), approaching the theoretical value of 59 mV for $n=1$ at 25°C. In contrast, slower electron transfer results in increased peak separation due to higher overpotential requirements. This principle serves as a valuable diagnostic tool for assessing the effectiveness of electrode modifications and for understanding charge transfer mechanisms in electrochemical systems (Mirceski et al., 2024; Raeisi-Kheirabadi et al., 2022). Therefore, the presence of sulfide-graphene nanoparticles on the electrode surface not only increases the active surface area but also improves the electron transfer rate. Another conclusion that can be drawn from Figures 3 and 4 is that a scan rate of 50 millivolts per second is the optimal rate for this study.

The voltammetric response (Curve α) shows a significant increase in oxidative current characteristics, evidenced by a 300% rise in peak amplitude and an expanded integrated peak area compared to the unmodified substrate. This notable current enhancement confirms the catalytic effectiveness of the cobalt disulfide-graphene nanocomposite, with the threefold increase in current directly linked to the electron mediation properties of the nanohybrid. These results are consistent with previous observations of accelerated charge transfer kinetics during ferrocyanide oxidation, indicating reliable catalytic behavior across various redox systems. The synergistic effects between the metallic sulfide and carbon nanostructure components improve both electron conduction and the electroactive surface area, ultimately contributing to the enhanced electrochemical performance (Saei and Asadpour-Zeynali, 2023).

Nanoparticles are essential as electrocatalysts in the electrochemical oxidation of hydrazine, as they greatly enhance the electron transfer rate. Their high surface-to-volume ratio and unique electronic properties promote faster charge transfer kinetics, resulting in more efficient electrochemical reactions. Additionally, nanoparticles increase the effective surface area of the electrode, offering more active sites for hydrazine oxidation. This expansion of the active surface area leads to a higher electrochemical current, indicating improved catalytic activity. The increase in current observed on nanoparticle-modified electrodes confirms their effectiveness in enhancing the electrochemical oxidation of hydrazine. This enhancement arises from both improved electron transfer efficiency and a greater number of available reaction sites. Consequently, the modified electrode demonstrates a stronger response to hydrazine oxidation compared to unmodified electrodes. Moreover, the amplified current response correlates with higher measurement sensitivity, enabling more precise and reliable detection of hydrazine. This improvement is especially advantageous in applications that require low detection limits, such as environmental monitoring, fuel cell technology, and chemical sensing. Thus, nanoparticle-modified electrodes present a promising strategy for optimizing electrochemical sensors and catalytic systems, combining enhanced reactivity with superior sensitivity. In summary, nanoparticles significantly enhance the electrocatalytic performance of electrodes by accelerating electron transfer, expanding the active surface area, and

increasing current response, ultimately improving sensitivity in hydrazine detection (Hatip et al., 2021; Miao et al., 2021; Wang et al., 2021).

The study concludes that the electrocatalytic oxidation of hydrazine on the modified electrode surface is controlled by diffusion. Initially, increasing the scan rate leads to a sharp rise in the anodic peak current, indicating a strong dependence on diffusion. However, as the scan rate continues to increase, the peak current rises more slowly, suggesting that diffusion is becoming the limiting factor. This behavior confirms that the reaction kinetics are determined by the mass transport of reactants to the electrode surface, rather than by the electron transfer process itself. The findings emphasize the crucial role of diffusion in influencing the efficiency of hydrazine oxidation at different scan rates (Alsoghier et al., 2024).

5. Conclusion

In conclusion, this study successfully engineered an advanced electrochemical transducer through functionalization with a cobalt sulfide-graphene nanocomposite, establishing a highly effective protocol for hydrazine sensing. The modified electrode demonstrated superior performance, evidenced by a significantly enhanced active surface area, a reduced peak potential separation (ΔE_p) confirming faster charge transfer kinetics, and exceptional stability with only a 3.8% current loss over 50 cycles. The sensor operated via a diffusion-controlled mechanism, as confirmed by Randles-Ševčík analysis, and achieved optimal electrocatalytic hydrazine oxidation at pH 9. The differential pulse voltammetry (DPV) method provided a highly sensitive and linear response ($R^2 = 0.998$) across a 0.2–2 mM concentration range, yielding a detection limit of 0.081 mM. This work validates the functionalized electrode as a robust, sensitive, and stable platform for reliable hydrazine quantification.

References

- Alsoghier, H. M., Abd-Elsabour, M., Alhamzani, A. G., Abou-Krishna, M. M., & Assaf, H. F. (2024). Real samples sensitive dopamine sensor based on poly 1,3-benzothiazol-2-yl ((4-carboxylicphenyl) hydrazono) acetonitrile on a glassy carbon electrode. *Scientific Reports*, *14*(1), 16601. <https://doi.org/10.1038/s41598-024-65192-0>
- Choi, H. N., Kim, H., Kim, M. J., & Sun, Y. K. (2024). Constructing the interconnected charge transfer pathways in sulfur composite cathode for all-solid-state lithium-sulfur batteries. *ACS Applied Materials & Interfaces*, *16*(8), 11076–11083. <https://doi.org/10.1021/acsami.3c18675>
- Fazeli-Nasab, B., Shahraki-Mojahed, L., Beigomi, Z., Beigomi, M., & Pahlavan, A. (2022). Rapid detection methods of pesticides residues in vegetable foods. *Chemical Methodologies*, *6*(1), 24–40. <https://doi.org/10.22034/chemm.2022.1.3>
- Golabi, S., Zare, H., & Hamzehloo, M. (2001). Electrocatalytic oxidation of hydrazine at a pyrocatechol violet (PCV) chemically modified

- electrode. *Microchemical Journal*, 69(2), 13–23. [https://doi.org/10.1016/s0026-265x\(00\)00158-2](https://doi.org/10.1016/s0026-265x(00)00158-2)
- Hatip, M., Koçak, S., & Dursun, Z. (2021). Sensitive determination of hydrazine using poly(phenolphthalein), Au nanoparticles and multiwalled carbon nanotubes modified glassy carbon electrode. *Turkish Journal of Chemistry*, 45(1), 167–180. <https://doi.org/10.3906/kim-2009-12>
- Herbei, E. E., Alexandru, P., & Busila, M. (2023). Cyclic voltammetry of screen-printed carbon electrode coated with Ag-ZnO nanoparticles in chitosan matrix. *Materials*, 16(8). <https://doi.org/10.3390/ma16083266>
- Huo, Y., Yu, T., Xue, Y., Zhang, G., Song, S., Shao, Y., & Han, X. (2024). Three CoS/CoO microspheres and their mixed matrix membranes for the highly efficient photocatalytic degradation of methyl blue. *RSC Advances*, 14(35), 25811–25819. <https://doi.org/10.1039/d4ra03261f>
- Iqbal, A. A., Harcen, C. S., & Haque, M. (2024). Graphene (GNP) reinforced 3D printing nanocomposites: An advanced structural perspective. *Heliyon*, 10(7), e28771. <https://doi.org/10.1016/j.heliyon.2024.e28771>
- Karami-Kolmoti, P., & Zaimbashi, R. (2023). An electrochemical sensing platform based on a modified carbon paste electrode with graphene/Co₃O₄ nanocomposite for sensitive propranolol determination. *ADMET & DMPK*, 11(2), 227–236. <https://doi.org/10.5599/admet.1705>
- Meng, J., Zahran, M., & Li, X. (2024). Metal-organic framework-based nanostructures for electrochemical sensing of sweat biomarkers. *Biosensors*, 14(10). <https://doi.org/10.3390/bios14100495>
- Miao, R., Yang, M., & Compton, R. G. (2021). The electro-oxidation of hydrazine with palladium nanoparticle modified electrodes: Dissecting chemical and physical effects—Catalysis, surface roughness, or porosity? *Journal of Physical Chemistry Letters*, 12(28), 6661–6666. <https://doi.org/10.1021/acs.jpcllett.1c01955>
- Michalkiewicz, S., Skorupa, A., Jakubczyk, M., & Bebacz, K. (2024). Application of a carbon fiber microelectrode as a sensor for apocynin electroanalysis. *Materials*, 17(7). <https://doi.org/10.3390/ma17071593>
- Mirceski, V., Guziejewski, D., & Gulaboski, R. (2024). Genuine anodic and cathodic current components in cyclic voltammetry. *Scientific Reports*, 14(1), 17314. <https://doi.org/10.1038/s41598-024-67840-x>
- Motaharian, A., & Milani, H. M. (2015). Electrochemical sensor based on molecularly imprinted polymer nanoparticles for determination of diazepam drug. *Journal of Applied Research in Chemistry*, 9(3), 51–59. <https://sid.ir/paper/180276/en>
- Najafi, M., & Sohuli, S. (2018). Electrochemical sensor for fentanyl determination by modified electrode with carbon nanotube and iron (III) oxide nanoparticles. *Journal of Applied Research in Chemistry*, 12(1), 103–110. <https://sid.ir/paper/180110/en>
- Nigde, M., Agir, I., Yildirim, R., & Isildak, I. (2022). Development and comparison of various rod-shaped mini-reference electrode compositions based on Ag/AgCl for potentiometric applications. *Analyst*, 147(3), 516–526. <https://doi.org/10.1039/d1an01754c>
- Ping, J., Wu, J., Wang, Y., & Ying, Y. (2012). Simultaneous determination of ascorbic acid, dopamine and uric acid using high-performance screen-printed graphene electrode. *Biosensors and Bioelectronics*, 34(1), 70–76. <https://doi.org/10.1016/j.bios.2012.01.016>
- Raeisi-Kheirabadi, N., Nezamzadeh-Ejhieh, A., & Aghaei, H. (2022). Cyclic and linear sweep voltammetric studies of a modified carbon paste electrode with nickel oxide nanoparticles toward tamoxifen: Effects of surface modification on electrode response kinetics. *ACS Omega*, 7(35), 31413–31423. <https://doi.org/10.1021/acsomega.2c03441>
- Saei, J. N., & Asadpour-Zeynali, K. (2023). Enhanced electrocatalytic activity of fluorine-doped tin oxide (FTO) by trimetallic spinel ZnMnFeO₄/CoMnFeO₄ nanoparticles as a hydrazine electrochemical sensor. *Scientific Reports*, 13(1), 12188. <https://doi.org/10.1038/s41598-023-39321-0>
- Sheikh-Mohseni, M. A., & Pirsas, S. (2016). Nanostructured conducting polymer/copper oxide as a modifier for fabrication of L-dopa and uric acid electrochemical sensor. *Electroanalysis*, 28(9), 2075–2080. <https://doi.org/10.1002/elan.201600089>
- Traipop, S., Jesadabundit, W., Khamcharoen, W., Pholsiri, T., Naorungroj, S., Jampasa, S., & Chailapakul, O. (2024). Nanomaterial-based electrochemical sensors for multiplex medicinal applications. *Current Topics in Medicinal Chemistry*, 24(11), 986–1009. <https://doi.org/10.2174/0115680266304711240327072348>
- Uzdrowska, K., Knap, N., Konieczna, L., Kamm, A., Kuban-Jankowska, A., Gieraltowska, J., ... Gorska-Ponikowska, M. (2025). Combined graphene oxide with 2-methoxyestradiol for effective anticancer therapy in vitro model. *International Journal of Nanomedicine*, 20, 933–950. <https://doi.org/10.2147/ijn.s498947>
- Wang, H., Dong, Q., Lei, L., Ji, S., Kannan, P., Subramanian, P., & Yadav, A. P. (2021). Co nanoparticle-encapsulated nitrogen-doped carbon nanotubes as an efficient and robust catalyst for electro-oxidation of hydrazine. *Nanomaterials*, 11(11). <https://doi.org/10.3390/nano11112857>
- Wang, L., Huang, P. F., Wang, H. J., Bai, J. Y., Zhang, L. Y., & Zhao, Y. Q. (2007). Covalent modification of glassy carbon electrode with aspartic acid for simultaneous determination of hydroquinone and catechol. *Annali di Chimica*, 97(5–6), 395–404. <https://doi.org/10.1002/adic.200790024>
- Wang, X., Wu, D., Yuan, D., & Wu, X. (2022). A nano-lead dioxide-composite electrochemical sensor for the determination of chemical oxygen demand. *Journal of Environmental Chemical Engineering*, 10(3), 107464. <https://doi.org/10.1016/j.jece.2022.107464>